

V. P. Lebedev, V. V. Lemanov, S. Ya. Misyura,
and V. I. Terekhov

UDC 532.526-536.24

The working surfaces are exposed to hot gas flows in many power plants. Thermal protection is provided by injecting a cooling gas along the surface. The extent of the cooling is governed by the performance in the gas injection, which is determined by the distribution for the relative dimensionless temperature of the adiabatic wall downstream from the injection point. It is familiar that gas injection gives good performance for low-turbulence flows [1]. Turbulent flow often occurs in actual plant. For example, in the combustion chamber in a gas turbine engine, the turbulence may attain 35% [2]. The turbulence has a substantial effect on the friction and heat transfer at the wall [2]. There is conflicting evidence on how elevated turbulence affects the protection. Some studies show that turbulent effects are marked, while others indicate that they are negligible. For example, in [3], the performance from slot injection was reduced by more than a factor of two, while in [4, 5] it was so by less than 30%. The reasons for the discrepancies may lie in the differing conditions. For example, in [3], the adiabatic surface was the wall of a metal tube, with the coolant injected near a turbulizing grid, in which a uniform flow did not arise, while the degree of turbulence was determined by calculation. Conflicting results may also arise from differences in initial turbulence. In [3-5], complete data are not given on the average and fluctuation characteristics in the part up to the working channel and at the inlet, so the results from different sources cannot be compared accurately. New experiments are required to supplement the performance data for various levels of turbulence and in order to elucidate the physics of the process.

We have examined how elevated turbulence in the incident flow affects the performance in slot gas injection.

The initial turbulence was varied widely. We made a detailed study on the flow parameters at the inlet: the distributions for the averaged and pulsating components of the velocity, and also the integral turbulence scale. We obtained evidence on how the turbulence intensity degenerates along the channel for various injection parameters. The method is given for considering how high external turbulence affects the calculation of gas injection performance.

The experiments were performed with a continuous-running aerodynamic tube (Fig. 1). The main parts were: 1 the divergent cone, 2 the equalizing grid, 3 the forechamber, 4 the turbulizer, 5 the convergent cone, 6 the separating insert, 7 the injection chamber, and 8 the cylindrical working section. In the convergent cone, the flow compression factor was $n = 7.2$. The working channel was made of Tufnol, internal diameter 80 mm and length 320 mm. The wall thickness in the cylindrical part was 20 mm. The injection was organized by an inlet gas chamber. At the inlet to the working section, there was an annular tangential slot of height 2 mm, through which the secondary gas flow was supplied. The separating insert was made of caprolon, thickness of separating edge 0.2 mm.

The following parameters were used: speed of main air flow $u_0 = 15$ m/sec, secondary flow injection parameter $m = \rho_s u_s / \rho_0 u_0 = 0.3-0.6$, turbulence intensity in the incident flow at the inlet to the working section $Tu_0 = \sqrt{\langle u'^2 \rangle} / u_0 = 0.2-15\%$, and temperatures of the main and injected gases $T_0 = 292$ K, $T_s = 360$ K correspondingly.

The temperature in the main flow was monitored with thermocouples at the axis of the forechamber. The temperature in the secondary flow was determined with thermocouples installed at the outlet from the injection chamber, while the temperature at the channel wall was measured with 19 chromel-copel thermocouples (of 0.2 mm diameter wire).

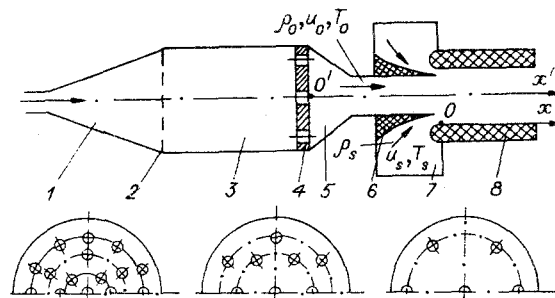


Fig. 1

The dynamic characteristics in the air flow were measured with a DISA 55M constant-temperature thermoanemometer, which was used with a standard 55M10 bridge, for which we used a single-filament 55P11 probe with filament diameter $8 \mu\text{m}$. The filament was perpendicular to the flow. The electrical quantities were converted to the velocity from [6]

$$E^2 = A + BU^n, \quad (1)$$

in which A and B were derived by least squares from the observed velocity U and voltage E. The errors in the E^2 derived from (1) and $n = 0.5$ (King's law) and $n = 0.4-0.6$ were virtually the same. King's formula was therefore used for the calibration.

The data were captured and processed for the temperature, mean velocity, turbulence, and other characteristics by means of a computerized system [7] consisting of the following major parts: the DISA Electronics thermoanemometer system, an IVK-2 data-acquisition suite containing an SM-4 minicomputer, an Elektronika-60 peripheral microcomputer, CAMAC apparatus, thermocouples, and a coordinate device. The thermoanemometer sensor was displaced with the two-component coordinate device, which provided a step of 0.02 mm.

We first examined the dynamic characteristics at the inlet from the velocity and pulsation pattern in the main flow with low turbulence intensity at the end of the slot. The patterns were very uniform (the maximum nonuniformity was 2%). We also measured the velocity profiles in the boundary layer in that section, which were closely described by a power law with parameter $1/n = 1/7$, which characterized developed boundary-layer turbulence. These measurements gave the displacement thickness for the boundary layer in the main flow at the end of the slot as 0.37 mm.

Elevated turbulence in the main flow was provided by turbulence generators consisting of disks with holes; Fig. 1 shows the scheme. The turbulizers were based on the [2] recommendations. Disk thickness, 4 mm, hole diameter $d = 10 \text{ mm}$. The two characteristic dimensions (hole diameter and distances between holes) are decisive for the turbulence scale. The degree of turbulence Tu was varied via the number of holes. The convergent cone also influences the turbulence scale, as it greatly deforms the largest vortices. The maximal turbulence intensity taken on the longitudinal velocity fluctuation component was 15% at the inlet, in spite of extensive pulsation suppression in the convergent cone. The compression in that cone resulted in uniform profiles for u_0 and Tu_0 at the edge of the slot. Measurements on the longitudinal fluctuation component at that edge gave the turbulence energy spectrum, which was free from discrete excursions. Those spectra gave the integral turbulence scale L. For $Tu_0 \approx 7-15\%$, $u_0 \approx 15 \text{ m/sec}$ we found $L \approx 6-10 \text{ mm}$, which corresponded to the characteristic turbulizer dimensions.

Figure 2 shows how the turbulence degenerates along the axis of the channel. The origin for the x' axis lies at the turbulizer (Fig. 1). The end of the slot in Fig. 2 corresponds to $x'/s = 132$. Points 1-4 show the variation in turbulence along the channel without gas injection for various initial Tu_0 with $u_0 = 15 \text{ m/sec}$, while points 5-8 are for injection. The points correspond to turbulizers with the following numbers of holes: points 1 and 5, seven holes, points 2 and 6, 13 holes, and 3 and 7, 25 holes. There is considerable degeneracy in the turbulence before the end of the slot. Further along the channel, Tu varies little. The minimum turbulence ($Tu \approx 0.2\%$) was provided by replacing the turbulizer by a grid, where Tu hardly varied along the channel (Fig. 2, lower graph). Figure 2 also shows that gas injection ($m \approx 0.6$) has little effect on the Tu distribution along the axis for various levels of initial turbulence.

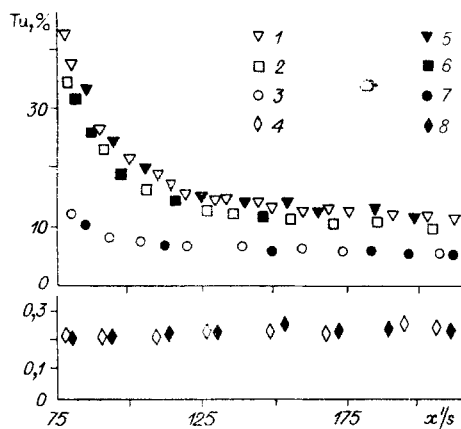


Fig. 2

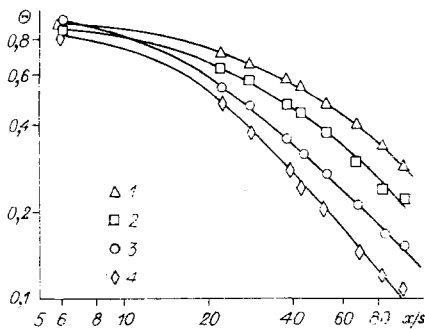


Fig. 3

TABLE 1

| Number of holes in turbulizer | Tu, % | C | X ₀ , m | N |
|----------------------------------|-------|--------|--------------------|-----|
| 25 | 7 | 1270,1 | 0,059 | 1,1 |
| 13 | 12 | 69,0 | 0,058 | 1,6 |
| 7 | 15 | 72,4 | 0,068 | 1,4 |

Most published studies on turbulence degeneration have been based on turbulence generators in the form of grids. In that case, the energy decay at short distances from the grid often corresponds [8] to

$$1/Tu^2 = C(X - X_0)^N \quad (2)$$

in which C, X₀, and N are constants. For a turbulizer of perforated washer type, as used here, it is difficult to choose the formula for the turbulence degeneration because a turbulizer of that type has several characteristic dimensions, each of which influences the Tu generation and degeneration. However, we found that (2) can be used for our data. Least-squares fitting gave the (2) coefficients for turbulizers with various numbers of holes. Table 1 gives the coefficients (the measured values were processed for x'/s ≈ 90-250).

The gas injection performance $\theta = (T_w - T_0)/(T_s - T_0)$ was determined from the measured wall temperature T_w. Figure 3 shows results for u₀ = 15 m/sec and m = 0.57 (Tu₀ = 0.2, 7, 12, 15%, points 1-4). As the turbulence increases from 0.2 to 15%, the slot injection performance deteriorates considerably throughout the length. Here θ decreases when the turbulence increases even slightly. For example, for Tu ≈ 7%, the points deviate considerably from those for Tu ≈ 0.2%. As the turbulence increases, the reduction in θ becomes more pronounced, e.g., by more than a factor of two for Tu ≈ 15% (by comparison with Tu ≈ 0.2%).

There is also a marked effect from Tu on the length of the initial section (Fig. 4), where points 1 and 2 correspond to m of 0.57 and 0.28, while points 3 show the [9] results. The initial part x₀ was determined from $\theta = f(x/s)$ (Fig. 3) from the intersection of $\theta = 1$ with the straight line drawn through the points, which fits them closely in logarithmic coordinates [10]. As the turbulence increases, that length decreases, and a similar effect has been found in a sheathed jet [9]. Our experiments showed that x₀ became more heavily dependent on Tu as the injection parameter increased. For example, with m = 0.57, a change in Tu from 0.2 to 15% reduced the length of the initial part by a factor of 2.5, as against only a factor of 1.4 for m = 0.28.

Figure 5 shows the measurements on the Tu effects in generalized coordinates. The points are as follows: 5) Tu₀ ≈ 0.2%, 6) 9% [4], 7) 15%, 8) 22% [3]. In those coordinates, the points for elevated turbulence lie below those for weak turbulence.

We used the Kutateladze-Leont'ev asymptotic boundary-layer theory [11] to describe the measurements. The performance in slot gas injection at an adiabatic wall is [11]

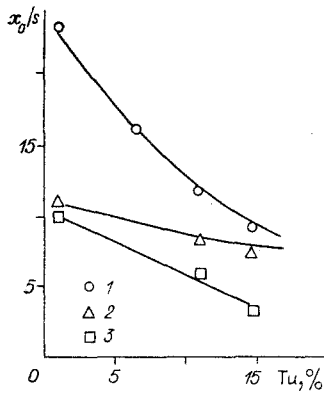


Fig. 4

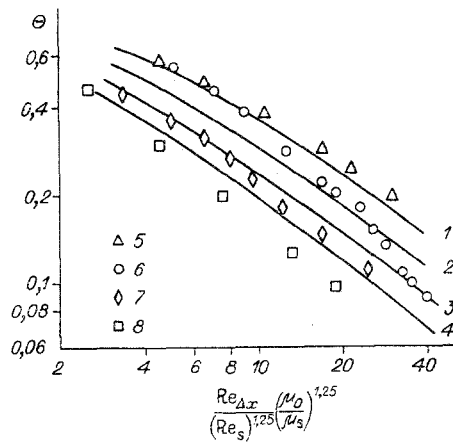


Fig. 5

TABLE 2

| Tu, % | 4 | 6 | 8 | 10 | 12 | 14 | 16 | 18 | 20 | 22 |
|---------|------|------|------|------|------|------|------|------|------|------|
| n | 7,2 | 8,1 | 8,9 | 9,8 | 10,7 | 11,5 | 12,4 | 13,2 | 14,1 | 15,0 |
| Ψ | 1,03 | 1,05 | 1,07 | 1,09 | 1,1 | 1,12 | 1,14 | 1,15 | 1,17 | 1,19 |
| β | 9,2 | 10,1 | 10,9 | 11,8 | 12,7 | 13,5 | 14,4 | 15,2 | 16,1 | 17,0 |
| A | 0,26 | 0,3 | 0,34 | 0,38 | 0,42 | 0,46 | 0,51 | 0,55 | 0,6 | 0,66 |

$$\Theta = \left[1 + A \frac{\text{Re}_{\Delta x}}{\text{Re}_s^{1,25}} \left(\frac{\mu_0}{\mu_s} \right)^{1,25} \right]^{-0,3}, \quad (3)$$

in which $A = 0.016\beta^{1.25}\Psi$; $\text{Re}_{\Delta x} = \rho_0 u_0 \Delta x / \mu_0$; $\text{Re}_s = \rho_s u_{s0} / \mu_s$; $\Delta x = x - x_0$. The coefficient $\beta = (\delta_{T^{**}})_{\text{ad}} / (\delta_{T^{**}})_{\Delta T = \text{const}}$ incorporates the temperature-pattern deformation when a boundary layer occurs at an adiabatic wall by comparison with the flow along a wall showing heat transfer. For $x \rightarrow \infty$, β tends to its maximum value [11]:

$$\beta \rightarrow \beta_{\text{max}} = \int_0^{\delta} \frac{\rho u}{\rho_0 u_0} dy \left/ \int_0^{\delta} \frac{\rho u}{\rho_0 u_0} \left(1 - \frac{T - T_w}{T_0 - T_w} \right) dy \right. \quad (4)$$

For an incompressible quasiisothermal flow, β is dependent on the velocity distribution in the boundary layer. Under standard conditions (gradient-free incompressible isothermal flow with low turbulence), the velocity profile is power-law form with parameter $1/n = 1/7$, while $\beta = 9$.

The relative heat-transfer function $\Psi = (\text{St}/\text{St}_0)_{\text{Re}_T}^{**}$ incorporates the change in the Stanton number due to perturbing factors under these conditions relative to the standard ones, where $\Psi = 1$. Under standard conditions, $A = 0.25$ in (3) with those values of β and Ψ . Then (3) with $A = 0.25$ ($\beta = 9$ and $\Psi = 1$) has been used to derive curve 1 in Fig. 5, which shows that the measurements fit that curve satisfactorily for low turbulence intensity.

With elevated turbulence, the velocity profile in the boundary layer is deformed. Measurements [2, 4, 12, 13] and our results suggest an interpolation expression for n , which is related to the turbulence:

$$n = n_0 + bTu \quad (5)$$

($n_0 = 5.5$, $b = 0.43$).

Elevated external turbulence accelerates heat transport in the boundary layer. Under those conditions, the relative heat-transfer function differs from unity and is [14] given by

$$\Psi = \Psi_{Tu} = 1 + 0,0085Tu. \quad (6)$$

With elevated turbulence, β in (3) should be determined on the basis of the change in the exponent in the velocity profile from (5), while Ψ is given by (6). Table 2 gives n , β , Ψ , and A derived from (4)-(6) for various Tu . The main effect from θ comes from β , while the effects from Ψ are slight over a wide range in Tu .

For points 7 in Fig. 5, we have $\beta \approx 14$, $\Psi \approx 1.13$, $A = 0.49$. Formula (3) gives curve 3 for those values of the coefficients, which describes the measurements satisfactorily.

Elevated turbulence reduces x_0 , but the effects of x_0 on $Re_{\Delta x}$ (particularly at large distances from the slot) are slight, and have been neglected in calculating the performance from (3). Here $A = 0.36$ in (3) in performance determination for $Tu_0 \approx 9\%$, and curve 2 in Fig. 5 shows (3) with $A = 0.36$. There are some discrepancies between the calculations and the points 6 because of the working conditions [4]. The injection there was with a long preceding dynamic section. For $Tu_0 \approx 22\%$, β and Ψ have been derived (Table 2) and have been used to construct curve 4. Figure 5 shows that the calculations in general reflect the experiments well.

When one corrects for how the turbulence affects the velocity profile and the heat transfer in (3), one can calculate the slot injection performance for a highly turbulent flow. Any more accurate description requires additional data on the turbulent characteristics, particularly the scale.

LITERATURE CITED

1. É. P. Volchkov, Wall Gas Injection [in Russian], Nauka, Novosibirsk (1983).
2. E. P. Dyban and É. Ya. Épik, Heat and Mass Transfer and Hydrodynamics in Turbulent Flows [in Russian], Naukova Dumka, Kiev (1985).
3. L. W. Carlson and E. Talmor, "Gaseous film cooling at various degrees of hot-gas acceleration and turbulence levels," *Int. J. Heat Mass Transfer*, 11, No. 11 (1968).
4. V. N. Vasechkin, B. P. Mironov, and N. I. Yarygina, The Performance from Pore and Slot Injection into Flows with Various Turbulence Levels [in Russian], Preprint No. 103, IT Akad. Nauk SSSR, Sib. Otd., Novosibirsk (1983).
5. V. V. Glazkov, M. D. Guseva, B. A. Zhestkov, and V. P. Lukash, "Effects of initial turbulence on the performance from permeable-wall cooling," *Inzh.-fiz. Zh.*, 39, No. 6 (1979).
6. J. O. Hinze, *Turbulence*, 2nd ed., McGraw-Hill, New York (1975).
7. V. V. Lemanov and S. Ya. Misyura, "Automating thermoanemometer measurements," in: *Automating Research in Thermophysics and Thermal Power Engineering* [in Russian], IT Sib. Otd. Akad. Nauk SSSR, Novosibirsk (1989).
8. J. C. Batchelor, *The Theory of Homogeneous Turbulence* [Russian translation], Izd. Inostr. Lit., Moscow (1955).
9. G. N. Abramovich, *Turbulent Jet Theory* [in Russian], Nauka, Moscow (1984).
10. R. A. Seban, "Heat transfer and effectiveness for a turbulent boundary layer with tangential fluid injection," *Trans. ASME, Ser. C*, No. 4 (1960).
11. S. S. Kutateladze and A. I. Leont'ev, *Heat and Mass Transfer and Friction in a Turbulent Boundary Layer* [in Russian], Énergoatomizdat, Moscow (1985).
12. A. Pyadishyus and A. Shlanchauskas, *Turbulent Heat Transfer in Wall Layers* [in Russian], Mokslas, Vilnius (1987).
13. G. Charnay, G. Comte-Bellot, and J. Mathieu, "Development of a turbulent boundary layer on a flat plate in an external turbulent flow," *Proc. AGARD Conf.*, No. 93, Paper 27 (1971), p. 27.1.
14. V. N. Mamonov, "Heat transfer on a permeable plate for an elevated degree of turbulence in the incident flow," in: *Turbulent Boundary Layers under Complicated Boundary Conditions* [in Russian], Nauka, Novosibirsk (1977).